Published in final edited form as:
Circulation. 2009 March 24; 119(11): 1501–1509. doi:10.1161/CIRCULATIONAHA.108.833327.

Early-life Sodium-exposure Unmasks Susceptibility to Stroke in hyperlipidemic-hypertensive Tg[hCETP]25-Rats

Julius L. Decano, MD[1,2], **Jason C. Viereck, MD,PhD**[3], **Ann C. McKee, MD**[3], **James A. Hamilton, PhD**[1,4], **Nelson Ruiz-Opazo, PhD**[1,2], and **Victoria L.M. Herrera, MD**[1,2]

[1]Whitaker Cardiovascular Institute, Boston University School of Medicine, Boston, Massachusetts, USA

[2]Department of Medicine, Boston University School of Medicine, Boston, Massachusetts, USA

[3]Department of Neurology, Boston University School of Medicine, Boston, Massachusetts, USA

[4]Department of Biophysics and Physiology, Boston University School of Medicine, Boston, Massachusetts, USA

Abstract

Background—Early-life risk factor exposure increases aortic atherosclerosis and blood pressure in humans and animal models, however, limited insight has been made into end-organ complications.

Methods and Results—We investigated the effects of early-life Na-exposure (0.23% *vs* 0.4%NaCl regular-rat chow) on vascular disease outcomes using the inbred, transgenic[hCETP]$_{25}$ Dahl salt-sensitive hypertensive rat model of male-predominant coronary atherosclerosis, Tg25. Rather than the expected increased coronary heart disease, fetal 0.4%Na-exposure (≤2g-Na/ 2000cal/diet/day) induced adult-onset stroke in both sexes (ANOVA $P<0.0001$), with earlier

*Correspondence to VLM Herrera, Whitaker Cardiovascular Institute, Room W-609, Boston University School of Medicine; 700 Albany Street, Boston, Massachusetts, USA 02118; vherrera@bu.edu; fax: 617-638-4066.

Conflict of Interest Disclosures
None.

Commentary:
Potential clinical impact – perspective for the practicing clinician
Despite major inroads into the treatment of hypertension and stroke, hypertension remains the leading risk factor for stroke, and stroke remains the 3rd leading cause of mortality. Validated animal models of stroke are needed for the identification of stroke mechanisms, hence elucidation of much-needed mechanism-based intervention and prevention strategies. The recently characterized rat stroke model, Tg25sp, provides several advantages. 1) As a model of spontaneous stroke that recapitulates two key risk factors, hypertension and hyperlipidemia, it provides an experimental system to investigate new targets for intervention and prevention strategies, as well as an animal model to test new drugs and diagnostic modalities with systematic histological corroboration. These critical tasks are impossible to do in human studies. 2) As a complex stroke model – spanning a spectrum of carotid artery disease, ischemic lesions, microhemorrhages, intraparenchymal hemorrhages, and microvascular alterations – stroke-prone Tg25sp rats prove, through reproducible modeling, that the association of these very same pathologies in humans is causally interrelated rather than just coincidence, thus giving experimental support for systematic study to determine prognosis for future stroke events. 3) As a model that exhibits strokes in females, Tg25sp rats provides a key experimental tool for the investigation of sex-specific mechanisms, and intervention and prevention strategies. 4) Most importantly, the demonstration of the impact of early-life Na exposure on adult-onset hypertension and stroke highlights the need for the study of Na-intake during gestation as a key prevention strategy. Current new studies fall short of the most vulnerable period for adult-onset stroke – in utero development.
and which affects females,
A priori, the recapitulation of risk factors for stroke is necessary in animal models of stroke. Foremost risk factors of stroke are hypertension, hyperlipidemia, and aging. The characterization of a new rat stroke model, Tg25sp rats provides a key additional experimental system to investigate pathogenic mechanisms of stroke, thereby identifying new targets for intervention and prevention strategies. Importantly, since stroke in Tg25sp rat model affects both females and males, it provides a critical model for studies of sex-specific mechanisms of stroke since the prototype rat stroke model only affected males.
model of stroke recapitulates two key risk factors

stroke-onset in Tg25-females. Analysis of later onsets of 0.4%Na-exposure resulted in decreased stroke-risk and later stroke-onsets, despite longer 0.4%Na-exposure durations, indicating increasing risk with earlier onsets of 0.4%Na-exposure. Histological analysis of stroke+rat brains revealed cerebral cortical hemorrhagic infarctions, microhemorrhages, neuronal ischemia, microvascular injury. Ex-vivo MRI of stroke+ rat brains detected cerebral hemorrhages, microhemorrhages and ischemia with middle cerebral artery-distribution, and cerebellar non-involvement. Ultrasound micro-imaging detected carotid artery disease. Pre-stroke analysis detected neuronal ischemia, and decreased mass of isolated cerebral, but not cerebellar, microvessels.

Conclusions—Early-life Na-exposure exacerbated hypertension and unmasked stroke susceptibility with greater female vulnerability in hypertensive-hyperlipidemic Tg25-rats. The reproducible modeling in Tg25sp rats of carotid artery disease, cerebral hemorrhagic-infarctions, neuronal ischemia, microhemorrhages, and microvascular alterations suggests a pathogenic spectrum with causal interrelationships. This “mixed-stroke” spectrum could represent paradigms of ischemic-hemorrhagic transformation, and/or a microangiopathic basis for the association of ischemic-lesions, microhemorrhages, and strokes in humans. Altogether, the data reveal early-life Na-exposure as a significant modifier of hypertension and stroke disease-course, hence a potential modifiable prevention target deserving systematic study.

Keywords

early-life Na-exposure; female-susceptibility; rat stroke model; microhemorrhages

Introduction

Coronary heart disease and stroke remain in the top three causes of death in the United Sates[1], despite clinical advances addressing their major risk factors, hypertension and hyperlipidemia[2]. This persistence mandates the study of pathogenic paradigms not addressed in current intervention and prevention approaches.

One such pathogenic paradigm is the impact of early-life risk-factor exposure on increasing susceptibility to adult-onset cardiovascular diseases3,[4]. Maternal hypercholesterolemia increases childhood (1–13 years) aortic atherosclerosis even in the presence of normocholesterolemia[5]. Likewise, maternal hyperglycemia increases risk for type-2 diabetes in humans6. Notably, effects of maternal hypercholesterolemia on atherosclerosis have been corroborated in controlled animal model studies: in rabbits7, in ApoE-knockout mice8 and in LDLr-knockout mice[9], while maternal environmental tobacco smoke exposure increased adult atherogenesis in ApoE-knockout mice[10]. However, we note that these studies did not analyze the impact on end-organ disease.

Analysis of the impact of early-life Na-exposure lags behind however, despite the significance of hypertension as a risk factor for coronary heart disease and especially stroke[11,12]. While intrauterine growth retardation and low birth weights have been found to be associated with hypertension in humans[13,14], epidemiology studies in humans studying the impact of common *in utero* exposures have not reported any maternal diet component to affect long-term offspring blood pressure[15]. Notably however, given that salt-sensitivity and salt-resistance are both present in patient populations, epidemiological detection of early-life Na-exposure effects will be difficult unless patients are stratified according to genetic predisposition to salt-sensitivity. Prior to successful genetic stratification of hypertension, animal model studies of human essential (polygenic) hypertension are necessary for the investigation of the role of early-life Na exposure effects on hypertension and its target-organ complications.

Studies in spontaneously hypertensive rats (SHRs) found that prenatal exposure to 5%Na-diet compared to 0.1%Na-diet, exacerbated hypertension at 4-months of age[16]. However, a similar study using 3%Na-diet found that hypertension was unchanged in 5- and 6-month old SHRs, which survived till 14–15 months of age, but that low 0.1%Na-diet prenatal exposure lowered BP significantly17. We note that all SHRs were maintained on 0.8%Na-diets from weaning16,17 with no reports of stroke occurrence. Not surprisingly, minimal effects were observed in Sprague-Dawley rats, an outbred normotensive strain, testing 3%Na-[18] and 8%Na-diet[19] prenatal exposures. However, these studies did not investigate the role of early-life Na-exposure on adult-onset, hypertensive end-organ diseases, which, given the importance of hypertension in exacerbating coronary heart disease[20] and in increasing risk for stroke[11,12], must be addressed.

The potential significance of the study of early-life risk factor exposure on 'adult-onset' disease course is high-impact, since early-life exposure which alters disease course is *a priori* a major confounder for genetic studies when unaccounted for. More importantly, elucidation of early-life modifiers of adult onset-disease pathogenesis given identical genetic predisposition, carries major health significance due to its potential efficacy, cost-effectiveness and accessibility as a target-mandate for prevention of adult-onset disease. Animal modeling studies are therefore needed that recapitulate the likely human clinical scenario – normotensive, normolipidemic mothers eating a balanced diet following current dietary sodium (2g-Na/2kCal-diet/day) recommendations, but whose offspring carry disease-susceptibility genotypes.

Here, we tested the hypothesis that in pre-hypertensive, normolipidemic dams, differential sodium intake affects disease course of adult-onset hypertension and vascular end-organ disease in genetically-predisposed offspring. Using the Tg[hCETP25-Dahl-S] transgenic rat model of polygenic-hypertension, hypercholesterolemia and hypertriglyceridemia with coronary atherosclerosis predominant in males (Tg25)[21], we investigated whether early-life Na-exposure will exacerbate coronary atherosclerosis through acceleration of salt-sensitive hypertension, just as differential adult-onset Na-exposure altered coronary atherosclerosis course22. Surprisingly, early-life 0.4%Na-exposure unmasked susceptibility to stroke in both Tg25-male and Tg25-female rats, with greater vulnerability in females despite equivalent blood pressure levels and less hyperlipidemia in Tg25-females compared to males.

Methods

Modeling early life Na-exposure effects on adult-onset vascular disease

We used heterozygous Tg25-rats, inbred Dahl salt-sensitive (Dahl S) rats transgenic for human cholesteryl ester transfer protein (CETP)[21] exposed to regular rat chow containing 0.4%Na (0.4%Na-exposure) at the desired experimental time point of onset: fetal (X_F), at weaning (X_W), and eight-weeks of age for early adulthood (X_A). Tg25-rats maintained on 0.23%Na-regular rat chow throughout life (C_F) served as reference[21]. All animal procedures were approved by the IACUC at Boston University School of Medicine. (Details and study group analysis sequence in the online-only Data Supplement)

Monitoring of Stroke Phenotype—Appearance of neurological deficits such as seizures, paralysis, and/or paresis defined stroke onset. (Details in the online-only Data Supplement).

Physiological and Biochemical Analyses—These were done as described[21] with more detail specified in the online-only Data Supplement.

Histopathology and Immunohistochemical Analyses—These were done as described[21] with more detail in the online-only Data Supplement.

Ex-vivo 11.7T Magnetic Resonance Imaging—Gradient-recalled echo sequence was used to assess hemorrhages and T2-weighted sequence was used to assess ischemia using an 11.7Tesla Avance 500 wide bore spectrometer (Bruker, Billerica MA). (Details in the online-only Data Supplement).

Ultrasound micro-imaging of rat carotid artery disease—Fifty-micron resolution ultrasound images were obtained using a Vevo770 imaging system (VisualSonics, Inc., Toronto CA). (Details in the online-only Data Supplement).

Isolation of Brain Microvessels (bmv)

Brain microvessels from rat cerebrum and cerebellum were isolated as described[23]. (Details in the online-only Data Supplement).

Statistical Analysis—All statistical analyses were done using Prism-4 (GraphPad Software Inc., La Jolla, CA). Details in the online-only Data Supplement.

Statement of Responsibility

The authors had full access to and take full responsibility for the integrity of the data. All authors have read and agree to the manuscript as written.

Results

Early life Na-exposure unmasks susceptibility to stroke

We investigated whether early-life sodium (Na)-exposure would exacerbate adult-onset cardiovascular disease in genetically salt-sensitive, hypertensive rats. We limited Na-exposure to fall within the range of standard salt levels contained in regular rat chow (0.23% to 0.4% NaCl) to simulate human dietary salt-intake. We note that 0.4% NaCl content is a time-tested, accepted level in regular rat chow, on which normal rat strains do not become hypertensive nor develop strokes. We also note that based on a typical rat intake of 20g/day equivalent to 100Cal/day[24], intake of 0.4%Na regular rat chow is equivalent to ≈1.6g-Na/2000Cal/day diet which complies with the recommended 2g-Na/2000Cal/day level for humans in the DASH diet25. To recapitulate the polygenic nature of human salt-sensitive hypertension, and eliminate genetic variability, we used the inbred, Tg25-transgenic rat model, which is a hyperlipidemic/polygenic hypertensive Dahl salt-sensitive rat model transgenic for human cholesteryl ester transfer protein21›26. To investigate whether onset of 0.4%Na-diet exposure is determinative, we studied effects of different onsets of 0.4%Na-exposure from conception (fetus, X_F), from 3-weeks (weanling, X_W), and from 8-weeks (adult, X_A) of age, compared with control rats on 0.23%Na-diet from conception (C_F). Differential impact on phenotype outcome of later 0.4%Na-exposure onsets despite equivalent or longer 0.4%Na-exposure durations would be informative as to the impact of early-life 0.4%Na-exposure.

Since Tg25-males have worse hypertension, hyperlipidemia and coronary atherosclerosis than age-matched Tg25-females which exhibit minimal if any coronary atherosclerosis[21], we expected that early-life Na-exposure would increase hypertension and exacerbate coronary artery disease in Tg25-males due to hypertension-atherosclerosis interactions as observed in the high expresser Tg[hCETP]53 rat line[22]. Surprisingly, X_F Tg25-male and female rats exhibited adult-onset stroke – marked by neurological deficits such as seizures, paresis and/or paralysis – compared to sex-matched C_F control rats (Figure 1A–B). Time

course analysis of early-life 0.4%Na-exposure revealed that X_W Tg25-males had less stroke-risk and later onset of stroke compared with X_F Tg25-males, despite longer duration of 0.4%Na-exposure in X_W Tg25-males (Figure 1-B). In females, time course analysis of 0.4%Na-exposure onsets showed that X_F and X_W Tg25-females exhibited similar stroke-risk and stroke-onsets, but that X_A Tg25-females exhibited decreased stroke risk and later stroke-onsets ($P<0.001$) despite almost 2-fold increase in 0.4%Na-exposure duration in X_A Tg25-female rats (Figure 1-A). Altogether, these observations indicate early-life vulnerability to 0.4%Na-exposure, with females showing a longer window of vulnerability to early-life 0.4%Na-exposure. The effects of early-life Na-exposure were corroborated by survival analysis of Tg25-males and females revealing $P < 0.0001$ for both respectively.

Two-way analysis of variance of early-life 0.4%Na exposure (X_F, X_W) and sex (Tg25-males, Tg25-females) demonstrate the relative significance and interaction of these two variables on stroke-onset. Early-life 0.4%Na-exposure contributed 21% of variance ($P<0.0001$), sex contributed 39% of variance ($P<0.0001$). Significant interaction of early-life 0.4%Na-exposure and sex contributed to 4.6% of stroke-onset variance ($P=0.0072$) (Supplemental Table 1). These data indicate significant sex-specific effects of early-life 0.4%Na-exposure on stroke-onset in Tg25-rats.

Sex-specific effects of early-life Na-exposure on hypertension

To gain further insight into determinants of the observed greater vulnerability of females to early-life Na-exposure induced adult-onset stroke, we investigated levels of hypertension and combined hyperlipidemia in age-matched X_F and C_F Tg25-male and female rats. Systolic blood pressure (SBP) analysis revealed equivalent levels between X_F Tg25-male and female rats at 2-, 3- and 4-months of age (Figure 1C; Supplemental Table 2). Notably however, analysis of increment rise in SBP at 2-, 3- and 4-month timepoints revealed significant differences between males and females (Figure 1C), suggesting that early-life Na-exposure exacerbated hypertension more in X_F Tg25-female rats, letting them ‘catch-up’ to the typically higher SBP levels in males. This observation is supported by two-way ANOVA of [early-life Na-exposure x sex] effects on SBP, which early-life Na-exposure contributing to 60% of SBP variance in females, compared to 15% in males (Figure 1C). Analysis of total plasma cholesterol and triglyceride levels of [X_F]Tg25-males and females detected significant differences between sexes at 2-, 3- and 4-months of age, but that females consistently had lower levels for both total plasma cholesterol and triglyceride levels (Figure 1D, Supplemental Table 2). We also note that levels observed were lower than previously reported[21].

Stroke phenotype characterization

To identify the stroke phenotype unmasked by early-life Na-exposure, multifaceted studies were done. Visual examination of the brains at the onset of stroke, marked by seizures, paresis and/or paralysis, revealed hemorrhages in different regions of the cerebral cortex, which were confirmed on histological analysis (Figure 2, A–F). Histological H&E-stained (data not shown) and Masson Trichrome-stained serial section analysis revealed acute hemorrhages (Figure 2, B and C) associated with neutrophil-adhesion and transmigration (Figure 3, A–C), as well as concurrent sub-acute hemorrhages characterized by hemorrhagic-necrotic areas with inflammatory cell infiltrates (Figure 2, E and F). Both acute and sub-acute hemorrhages were associated with microhemorrhages which were mostly found in the cerebral cortex (Figure 2, A–F), as well as in the hippocampus, basal ganglia and white matter.

Areas surrounding cerebral microhemorrhages showed evidence of ischemia with neuronal pyknosis, eosinophilia and microvacuolation in the surrounding tissue (Figure 3, D and E),

in contrast to non-affected areas (Figure 3F). Microvessels exhibiting microhemorrhages also exhibited endothelial denudation (Figure 3A), and discontinuous glial fibrillary acidic protein (GFAP)-positive astrocytic endfeet (Figure 4, A–C), concordant with post-ischemic loss of microvascular integrity[27].

Interestingly, neutrophil-transmigration without red blood cell extravasation and perivascular edema (Figure 3, A and B) was observed, concordant with previous observations of neutrophil recruitment prior to loss of microvascular integrity[28]. Transmigrated neutrophils immunostained positively for myeloperoxidase (Figure 3B), concordant with the concept that post-ischemic neutrophil transmigration might promote further vascular injury and lead to additional and/or larger hemorrhage (Figure 3C) via myeloperoxidase-H_2O_2-halide system-induced toxicity[29]. Areas of subacute hemorrhagic infarction also exhibited positive myeloperoxidase immunostaining (Figure 4D) in the neuropil (Figure 4E), as well as in monocytes and macrophages (Figure 4F), suggesting continued myeloperoxidase-mediated tissue injury after the 48-hour post-ischemic period. Compared to age-matched pre-stroke and non-stroke prone C_FTg25-female rats, we detected increased circulating CD11b+ activated neutrophils ($P<0.0001$, Figure 5, A–C) and plasma interleukin-18 levels ($P<0.0001$, Figure 5D) at the onset of neurological deficits in stroke +Tg25-female rats, suggesting a systemic pro-inflammatory process in post-ischemic hemorrhagic transformation.

Histological time-course analysis of stroke-prone rat brains

Comparative microscopic examination of rat study groups detected acute macrohemorrhages, subacute hemorrhagic-necrotic lesions, and neutrophil recruitment only at the onset of stroke-associated neurologic deficits (Supplemental Table 3). Microhemorrhages were mainly detected at stroke onset, and occasionally in 2 and 3 month-old Tg25-females, but not in Tg25-males of similar ages (Supplemental Table 3), consistent with the observations that stroke occurs later in males (Figure 1, A and B). Features of acute ischemia, such as neuronal pyknosis and eosinophilia, were detected at pre-stroke time points suggesting that ischemia likely precedes microhemorrhages (Supplemental Table 3).

Magnetic Resonance Imaging (MRI) Analysis of Stroke+ Brains

To further characterize the stroke phenotype, we applied 32 micron/pixel-resolution MRI at 11.7Tesla to fixed rat brains. Using a gradient-recalled echo sequence which detects heme products, MR-imaging detected multiple cortical intraparenchymal microhemorrhages, and larger hemorrhages in the subcortical white matter (Figure 6A). Gradient-recalled echo MRI also detected microhemorrhages in the hippocampus and thalamus (data not shown). Analysis of T2-weighted images detected a relatively extensive region of abnormal, high signal (Figure 6B). Quantification of intensity of T2-weighted imaging, highlighting pixels with intensity above 70% of maximal signal, better delineated the high-signal area, consistent with ischemia with a middle cerebral artery distribution (Figure 6C), thus revealing that microhemorrhages occurred within ischemic tissue. Together with histological observations, the MRI findings of multiple, mixed cortical and white matter hemorrhages, and microhemorrhages within middle-cerebral artery ischemic distribution demonstrate the stroke phenotype in Tg25sp model as ischemic-hemorrhagic stroke.

Ultrasonographic detection of carotid artery atherosclerosis

To investigate the cause of the ischemia following middle artery distribution detected on ex vivo MRI, we used a 50-micron resolution ultrasound system to investigate putative carotid artery disease at the onset of stroke in another set of X_F rats. Ultrasonography detected carotid artery disease in the internal carotid artery (Figure 7), or at the carotid bifurcation and ruled-out concomitant heart failure (data not shown). These observations support the

MRI findings of ischemia with middle cerebral artery distribution and suggest that stroke pathogenesis in this model likely involves the synergistic interactions of embolic and low flow hemodynamic factors known to be contributory to stroke pathogenesis in large artery atherosclerotic disease[30].

Pre-stroke brain changes in microvascular mass

In order to investigate the hypothesis that pre-stroke changes exist in brain microvessels (bmv) which increase ischemic damage and risk for hemorrhagic transformation, we investigated putative pre-stroke changes in brain microvessels. At the onset of stroke, histological, serial-section analysis of cortical areas with ischemic neurons demonstrated decrease in the number of brain microvessels (bmv) – zero to one per 1000x-high power field (Figure 3, D and E), in contrast to non-ischemic cortical areas on the same section which exhibit two to three brain microvessels per 1000X-high power field (Figure 3F). To assess putative pre-stroke changes in brain microvessel density, we isolated brain microvessels (bmv) (Figure 5, E and F) comparing different study groups and pre-stroke time points. The study of bmv-mass gives a total representative picture of bmv status in specific brain regions.

In pre-stroke rats at 4 to 4.5 months of age, cerebral cortical microvessel density, measured as cortical bmv-mass/cortex weight, was significantly different among age-matched X_F-females, X_A- females and X_F-males (Figure 5G). Interestingly, analysis of total cerebral cortical microvessel density at earlier time points, 2 and 3 months of age, did not detect differences in X_F-study groups, respectively (data not shown). Concordant with the absence of cerebellar lesions, cerebellar brain microvessel number is not altered among study groups (data not shown).

Discussion

Early-life 0.4%Na-exposure unmasks stroke susceptibility with greater female vulnerability

Early-life 0.4%Na-exposure unmasks susceptibility to adult-onset stroke in Tg25-rats, in contrast to later-life 0.4%Na-exposure despite longer durations of 0.4%Na-exposure in the latter. Without early-life 0.4%Na-exposure, Tg25-females and males did not exhibit adult-onset stroke[21]. We note however, that genetic susceptibility to hypertension plays a critical role in early-life 0.4%Na-exposure-induced stroke susceptibility, since lifetime 0.4%Na-Purina 5001 rat chow consumption does not induce strokes in other rat strains including SHR strain. These observations highlight the importance of gene-environment interactions and the impact of early-life exposure on disease course in genetically predisposed individuals. The data also demonstrate the role of sex-specific factors since, given identical early-life Na-exposure, genetic backgrounds, similar levels of blood pressure, and less hyperlipidemia, Tg25-females exhibited earlier onsets of stroke and a longer window of vulnerability to early-life Na-exposure induced risk for adult-onset stroke compared with Tg25-males.

Modeled paradigms in the stroke-prone Tg25 (Tg25sp) rat model

The detection of hemorrhagic infarctions, carotid artery disease and artery-specific ischemic distribution encompassing multiple microhemorrhages and intraparenchymal hemorrhages, and microvascular pathology altogether recapitulate human ischemic-embolic strokes with hemorrhagic transformation, the clinical association of microhemorrhages and ischemic stroke[31], and the coexistence of microangiopathy, microhemorrhages and acute spontaneous intraparenchymal hemorrhage in humans[32]. The reproducible modeling of these features in the inbred Tg25sp rat model provides compelling evidence that these events are

pathogenically interrelated, and supports the hypothesis that carotid artery disease embolic and hemodynamic events act synergistically to increase stroke risk[30].

More importantly, the modeling of spontaneous carotid artery disease and ischemic stroke with hemorrhagic transformation in X_F0.4%Na-exposed Tg25-rats, or stroke-prone Tg25sp rats, affecting both females and males, provides a much needed new animal model of spontaneous, ischemic-stroke with hemorrhagic transformation. This stroke-model provides the biological context of clinically relevant stroke-risk factors, polygenic hypertension and hyperlipidemia, which are missing in commonly used stroke models induced by the acute-injection of blood or collagenase[33,34], or acute arterial ligation- or microsphere-induced ischemia[35,36]. As such, the Tg25sp model provides a compelling model system to analyze pre-stroke changes leading to ischemic strokes, post-ischemic hemorrhagic transformation, and progression of microhemorrhages to intraparenchymal hemorrhages.

Additionally, the Tg25sp stroke model differs from the prototype stroke-prone SHRsp rat stroke-model since the latter exhibits hypertensive arterial fribrinoid necrosis, greater male susceptibility[37,38], and distinct vascular, neuronal and parenchymal histopathological changes[39,40]. Given that women are reported to have more strokes than men in 2004 with 91,274 deaths from strokes in females compared to 58,800 deaths in males[41], the fact that the Tg25sp rat model recapitulates this trend, validates Tg25sp rats as a model system to study sex-specific stroke-mechanisms and test corresponding sex-specific stroke-intervention approaches.

Implication of a brain microvascular paradigm in stroke pathogenesis

The pre-stroke decrease in microvascular-mass, microvascular paucity associated with neuronal ischemia, loss of endothelial integrity and astrocyte-endfeet contiguity collectively implicate a microvascular-paradigm which could contribute to continuing cycles of microvascular dysfunction-ischemia after the initial ischemic stroke event. Coupled with IL-18 mediated activation of neutrophils, neutrophil transmigration and myeloperoxidase release, microvascular paucity and dysfunction could lead to increased susceptibility for ischemic hemorrhagic transformation. Altogether, these observations support the hypothesis that a hemorrhage-prone angiopathy underlies multiple cerebral microhemorrhages[42], which upon progression, could underlie the observed coexistence of microhemorrhages with acute intraparenchymal hemorrhages in humans[32] and the predictive association of microhemorrhages with new and/or fatal strokes in patients with ischemic strokes[43]. These multiple concordances between Tg25sp-model and clinical observations support a microvascular-paradigm in stroke pathogenesis.

Study Limitations

Observations are currently limited to rat modeling wherein hypertension is not treated at SBP>160mmHg, and hyperlipidemia is due to CETP-transgenic expression in a susceptible genetic background. Despite severe hypertension, the Tg25sp rat model of stroke does not exhibit cerebellar hemorrhages, which is a feature of hypertensive hemorrhagic strokes in humans. While the data reveal a microvascular-paradigm in stroke pathogenesis, investigation of impact of early-life Na-exposure on the kidney and carotid artery vascular wall will be necessary. Additionally, future studies will be required to elucidate mechanisms underlying observed sex-specific differences. We qualify that the observation of strokes rather than coronary heart disease does not imply non-importance of Na-exposure to coronary heart disease, since strokes occurred much earlier than the expected onset of pathogenesis of coronary heart disease in this model.

Clinical Implications and Conclusions

In summary, our findings demonstrate that early-life Na-exposure within levels complying with current recommended daily sodium intake[25], is a key modifier of hypertension and its target-organ complications in genetically predisposed individuals, and reveals greater susceptibility in females. When unaccounted for, changes in disease course induced by differential early-life Na-exposure will confound genetic analyses of adult-onset hypertension and hypertensive end-organ complications. Such confounders most likely underlie the shortfall in identifying hypertension and/or stroke susceptibility genes despite large cohort-studies[44].

The modeling of cerebral microvascular abnormalities, microhemorrhages, hemorrhagic infarction and intraparenchymal hemorrhages as a spectrum suggests pathogenic interrelationships, which given the new Tg25sp rat stroke model, can now be systematically investigated as to mechanism(s), and as to new diagnostic and therapeutic approaches. The use of clinically pertinent diagnostic modalities – MRI and ultrasound carotid-artery imaging, FACS analysis and circulating biomarkers – and the correlation of these findings with molecular and histopathological observations in Tg25sp rats could facilitate clinical translation of model-derived mechanistic insight. Most importantly, given that stroke risk persists despite successful anti-hypertensive therapies[2], the data support the mandate for further study of early-life Na-exposure as a potential high-impact prevention target to decrease adult-onset hypertension and strokes.

Supplementary Material

Refer to Web version on PubMed Central for supplementary material.

Acknowledgments

Funding Sources

This work was supported by NIH-ES013870 and NIH-AG032649 to V.L.M. Herrera.

REFERENCES

1. Heart Disease and Stroke Statistics – 2008 Update. American Heart Association.org. 2008
2. Dahlof B. Prevention of stroke in patients with hypertension. Am J Cardiol 2007;100(suppl):17J–24J.
3. Gluckman PD, Hanson MA, Cooper C, Thornburg KL. Effect of in utero and early-life conditions on adult health and disease. N Engl J Med 2008;359:61–73. [PubMed: 18596274]
4. Palinski W, Yamashita T, Freigang S, Napoli C. Developmental programming: maternal hypercholesterolemia and immunity influence susceptibility to atherosclerosis. Nutr Rev 2007;65(12 Pt 2):S182–S187. [PubMed: 18240546]
5. Napoli C, Glass CK, Witztum JL, Deutsch R, D'Armiento FP, Palinski W. Influence of maternal hypercholesterolemia during pregnancy on progression of early atherosclerotic lesions in childhood: fate of early lesions in children (FELIC) study. Lancet 1999;354:1234–1241. [PubMed: 10520631]
6. Dabelea D, Hanson RL, Lindsay RS, Pettitt DJ, Imperatore G, Gabir MM, Roumain J, Bennett PH, Knowler WC. Intrauterine exposure to diabetes conveys risks for type 2 diabetes and obesity: a study of discordant sibships. Diabetes 2000;49:2208–2211. [PubMed: 11118027]
7. Napoli C, Witztum JL, Calara F, de Nigris F, Palinski W. Maternal hypercholesterolemia enhances atherogenesis in normocholesterolemic rabbits which is inhibited by antioxidant or lipid-lowering intervention during pregnancy: an experimental model of atherogeneic mechanisms in human fetuses. Circ Res 2000;87:946–952. [PubMed: 11073892]
8. Alkemade FE, Gittenberger-de Groot AC, Schiel AE, VanMunsteren JC, Hogers B, vanVliet LSJ, Poelmann RE, Havekes LM, vanDijk KW, DeRuiter MC. Intrauterine exposure to maternal

atherosclerotic risk factors increases the susceptibility to atherosclerosis in adult life. Arterioscler Thromb Vasc Biol 2007;27:2228–2235. [PubMed: 17656671]

9. Napoli C, de Nigris F, Welch JS, Calara FB, Stuart RO, Glass CK, Palinski W. Maternal hypercholesterolemia during pregnancy promotes early atherogenesis in LDL receptor-deficient mice and alters aortic gene expression determined by microarray. Circulation 2002;105:1360–1367. [PubMed: 11901049]
10. Yang Z, Knight CA, Mamerow MM, Vickers K, Penn A, Postlethwait EM, Ballinger SW. Prenatal environmental tobacco smoke exposure promotes adult atherogenesis and mitochondrial damage in apolipoprotein E−/− mice fed a chow diet. Circulation 2004;11:3715–3720. [PubMed: 15569831]
11. Messerli FH, Williams B, Ritz E. Essential hypertension. Lancet 2007;370:591–603. [PubMed: 17707755]
12. Iadecola C, Davisson RL. Hypertension and cerebrovascular dysfunction. Cell Metabolism 2008;7:476–484. [PubMed: 18522829]
13. Barker D, Bull A, Osmond C, Simmonds S. Fetal and placental size and risk of hypertension in adult life. BMJ 1990;310:259–262. [PubMed: 2390618]
14. Law CM, de Swiet M, Osmond C, Fayers PM, Barker DJP, Cruddas AM, Fall CHD. Initiation of hypertension in utero and its amplification throughout life. BMJ 1993;306:24–27. [PubMed: 8435572]
15. Brion MJ, Leary SD, Lawlor DA, Smith GD, Ness AR. Modifiable maternal exposures and offspring blood pressure: a review of epidemiological studies of maternal age, diet and smoking. Pediatr Res 2008;63:593–598. [PubMed: 18317238]
16. Nicolantonio RD, Spargo S, Morgan TO. Prenatal high salt diet increases blood pressure and salt retention in the spontaneously hypertensive rat. Clin Exp Pharmacol Physiol 1987;14:233–235. [PubMed: 3665192]
17. Di Nicolantonio R, Hoy K, Spargo S, Morgan TO. Perinatal salt intake alters blood pressure and salt balance in hypertensive rats. Hypertension 1990;15:177–182. [PubMed: 2303281]
18. Contreras RJ, Wong DL, Henderson R, Curtis KS, Smith JC. High dietary NaCl early in development enhances mean arterial pressure of adult rats. Physiol Behav 2000;71:173–181. [PubMed: 11134699]
19. Porter JP, King SH, Honeycutt AD. Prenatal high-salt diet in the Sprague Dawley rat programs blood pressure and heart rate hyperresponsiveness to stress in adult female offspring. Am J Physiol Regul Integr Comp Physiol 2007;293:R334–R342. [PubMed: 17491116]
20. MRFIT: Multiple Risk Factor Intervention Trial Research Group. Relationship between baseline risk factors and coronary heart disease in Multiple Risk Factor Intervention Trial. Prev Med 1986;15:254–273. [PubMed: 3749007]
21. Herrera VLM, Tsikoudakis A, Didishvili T, Ponce LRB, Bagamasbad P, Gantz D, Herscovitz H, Van Tol A, Ruiz-Opazo N. Analysis of gender-specific atherosclerosis susceptibility in transgenic[hCETP]25^{DS} rat model. Atherosclerosis 2004;177:9–18. [PubMed: 15488860]
22. Herrera VLM, Didishvili T, Lopez LV, Zander K, Travers S, Gantz D, Herscovitz H, Ruiz-Opazo N. Hypertension exacerbates coronary artery disease in transgenic hyperlipidemic Dahl salt-sensitive hypertensive rats. Mol Med 2001;7:831–844. [PubMed: 11844871]
23. Song L, Pachter JS. Culture of murine brain microvascular endothelial cells that maintain expression and cytoskeletal association of tight junction-associated proteins. In Vitro Cell Dev Biol Anim 2003;39:313–320. [PubMed: 14613336]
24. Contreras, RJ. Influence of Early Salt Diet on Taste and Blood Pressure. In: Hyson; Johnson, editors. The Biology of Early Influences. New York: Kluwer Academic/Plenum Publishers; 1999.
25. Sacks FM, Svetkey LP, Vollmer WM, Appel LJ, Bray GA, Harsha D, Obarzanek E, Conlin PR, Miller ER, Simons-Morton DG, Karanja N, Lin PH. DASH-sodium collaborative research group. Effects on blood pressure or reduced dietary sodium and the dietary approaches to stop hypertension (DASH) diet. NEJM 2001;344:3–10. [PubMed: 11136953]
26. Herrera VLM, Makrides S, Xie HX, Adari H, Krauss RM, Ryan U, Ruiz-Opazo N. Spontaneous combined hyperlipidemia, coronary heart disease and decreased survival in Dahl salt-sensitive

hypertensive rats transgenic for human cholesteryl ester transfer protein. Nature Med 1999;5:1383–1389. [PubMed: 10581080]

27. del Zoppo GJ, Hallenbeck JM. Advanced in the vascular pathophysiology of ischemic stroke. Thrombosis Research 2000;98:V73–V81.
28. Hallenbeck JM, Dutka AJ, Tanishima T, Kochanek PM, Kumaroo KK, Thompson CB, Obrenovitch TP, Contreras TJ. Polymorphonuclear leukocyte accumulation in brain regions with low blood flow during the early postischemic period. Stroke 1986;17:246–253. [PubMed: 3961835]
29. Klebanoff SJ. Myeloperoxidase: friend and foe. J Leukocyte Biol 2005;77:598–625. [PubMed: 15689384]
30. Derdeyn CP. Mechanisms of ischemic stroke secondary to large artery atherosclerotic disease. Neuroimag Clin N Am 2007;17:303–311.
31. Werring DJ, Coward LJ, LOsseff NA, Jager HR, Brown MM. Cerebral microbleeds are common in ischemic stroke but rare in TIA. Neurology 2005;65:1914–1918. [PubMed: 16380612]
32. Alemany M, Stenborg A, Terent A, Sonninen P, Raininko R. Coexistence of microhemorrhages and acute spontaneous brain hemorrhage: correlation with signs of microangiopathy and clinical data. Radiology 2006;238:240–247. [PubMed: 16373772]
33. Andaluz N, Zuccarello M, Wagner KR. Experimental animal models of intracerebral hemorrhage. Nuerosurg Clin N Am 2002;13:385–393.
34. MacLellan CL, Silasi G, Poon CC, Edmundson CL, Buist R, Peeling J, Colbourne F. Intracerebral hemorrhage models in rat: comparing collagenase to blood infusion. J Cereb Blood Flow Metab 2008;28:516–525. [PubMed: 17726491]
35. Carmichael ST. Rodent models of focal stroke: size, mechanism, and purpose. J Am Soc Exp NeuroTher 2005;2:396–409.
36. Durukan A, Tatlisumak T. Acute ischemic stroke: overview of major experimental rodent models, pathophysiology, and therapy of focal cerebral ischemia. Pharmacol Biochem Behav 2007;87:179–197. [PubMed: 17521716]
37. Sironi L, Guerrini U, Tremoli E, Miller I, Gelosa P, Lascialfari A, Zucca I, Eberini I, Gemeiner M, Paoletti R, Gianazza E. Analysis of pathological events at the onset of brain damage in stroke-prone rats: a proteomics and magnetic resonance imaging approach. J Neurosci Research 2004;78:115–122. [PubMed: 15372505]
38. Ballerio R, Gianazza E, Mussoni L, Miller I, Gelosa P, Guerrini U, Eberini I, Gemeiner M, Belcredito S, Tremoli E, Sironi L. Gender differences in endothelial function and inflammatory markers along the occurrence of pathological events in stroke-prone rats. Exp Mol Pathology 2007;82:33–41.
39. Fredriksson K, Kalimo H, Nordborg C, Johansson BB, Olsson Y. Nerve cell injury in the brain of stroke-prone spontaneously hypertensive rats. Acta Neuropathol 1988;76:227–237. [PubMed: 3213425]
40. Fredriksson K, Nordborg C, Kalimo H, Olsson Y, Johansson BB. Cerebral microangiopathy in stroke-prone spontaneously hypertensive rats: an immunohistochemical and ultrastructural study. Acta Neuropathol 1988;75:241–252. [PubMed: 3348082]
41. U.S. National Center for Health Statistics 2007. Centers for Disease Control and Prevention, US Department of Health and Human Services. <http://www.cdc.gov/nchs>
42. Lee SH, Bae HJ, Kwon SJ, Kim H, Kim YH, Yoon BW, Roh JK. Cerebral microbleeds are regionally associated with intracerebral hemorrhage. Neurology 2004;62:72–76. [PubMed: 14718700]
43. Boulanger JM, Coutts SB, Eliasziw M, Gagnon AJ, Simon JE, Subramaniam S, Sohn CH, Scott J, Demchuk AM. for the VISION Study Group. Cerebral microhemorrhages predict new disabling or fatal strokes in patients with acute ischemic stroke or transient ischemic attack. Stroke 2006;37:911–914. [PubMed: 16469961]
44. The Wellcome Trust Case Control Consortium. Genome-wide association study of 14,000 cases of seven common diseases and 3,000 shared controls. Nature 2007;447:661–678. [PubMed: 17554300]

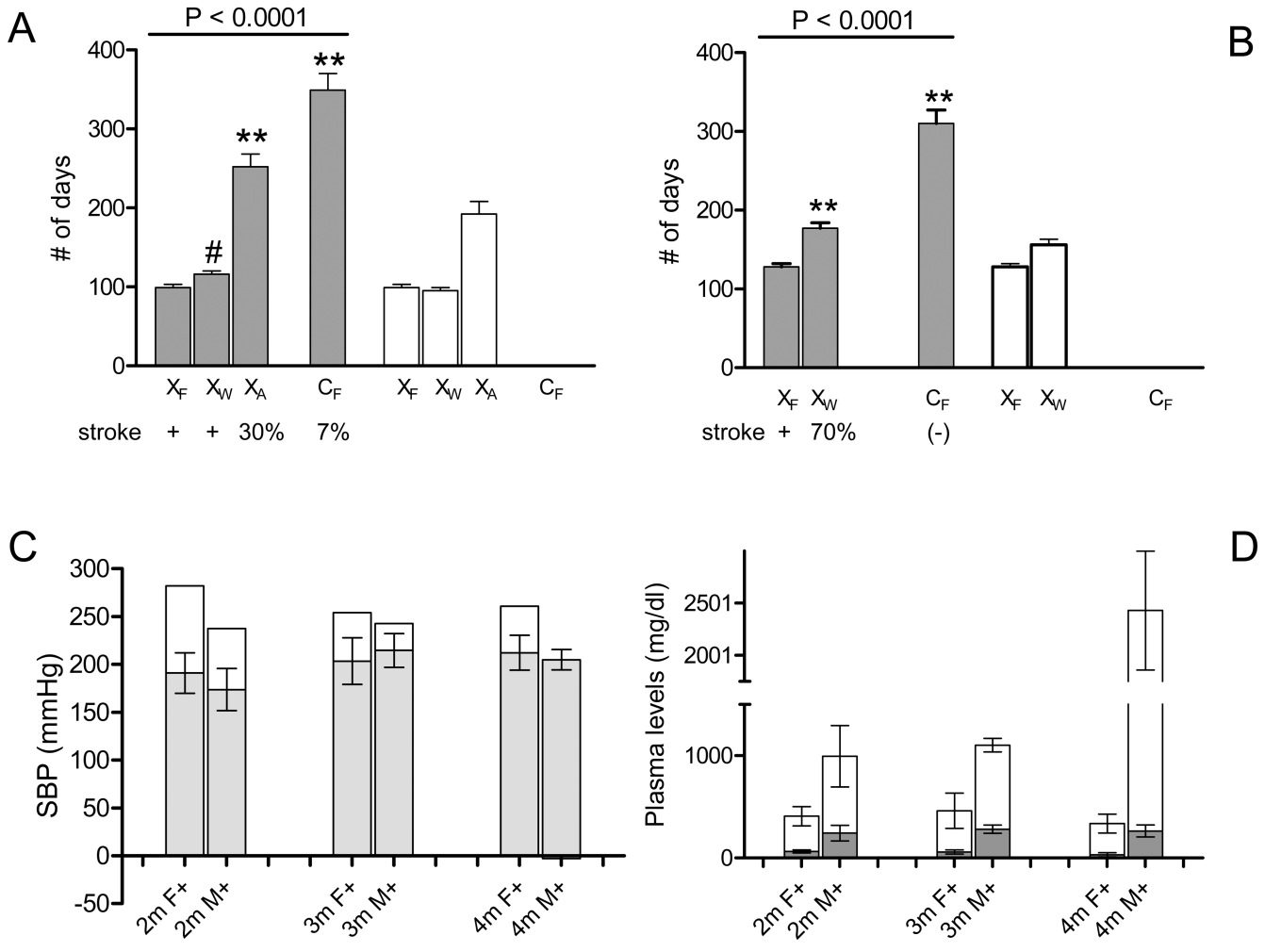

Figure 1.

Early-life 0.4%Na-exposure effects on stroke onset and hypertension in Tg25-female and male rats.

(A) Lifespan ■ and Na-exposure duration □ in Tg25-females per study group: X_F, X_W, X_A, and control C_F. Strokes were observed (+) in X_F and X_W, and much later and in fewer (30%) X_A rats, and even much later and in fewer (7%) C_F rats[21]. Mean ± sem; ANOVA $P<0.0001$; **, Tukey's Multiple Comparison $P<0.001$ vs X_F; #, not significant.

(B) Lifespan ■ and Na-exposure duration □ in Tg25-males per study group: X_F, X_W, and control C_F. Strokes were observed (+) in X_F males, and in 70% of X_W males with later onsets, but not in C_F rats[21]. Mean ± sem; ANOVA $P<0.0001$; **, Tukey's Multiple Comparison $P<0.001$ vs X_F.

(C) Systolic blood pressure (SBP) level in mmHg, ■, in X_F Tg25-females (F+) and males (M+) at 2m, 3m, and 4m of age (paired t-test $P>0.3$); mean ± sd. Corresponding increment rise in mean SBP, □, in X_F rats compared with C_F rats (X_F - C_F) at 2m, 3m and 4m: (paired t-test $P<0.03$). Two-way ANOVA: early life Na-exposure contributes to 60% of SBP variance in females ($P<0.0001$), 15% of SBP variance in males ($P<0.0001$).

(D) Plasma levels (mean±sd) of total plasma cholesterol, TC, (■) and total plasma triglyceride, TG, levels (□) of X_F rats at 2m-, 3m- and 4-months of age (paired t-test

$P<0.001$ for each timepoint respectively). For total plasma triglyceride levels, Tukey's Multiple Comparison test at 2m: $P<0.05$; for 3m: $P<0.01$; for 4m: $P<0.001$. (Date specifics in the online-only Data Supplement).

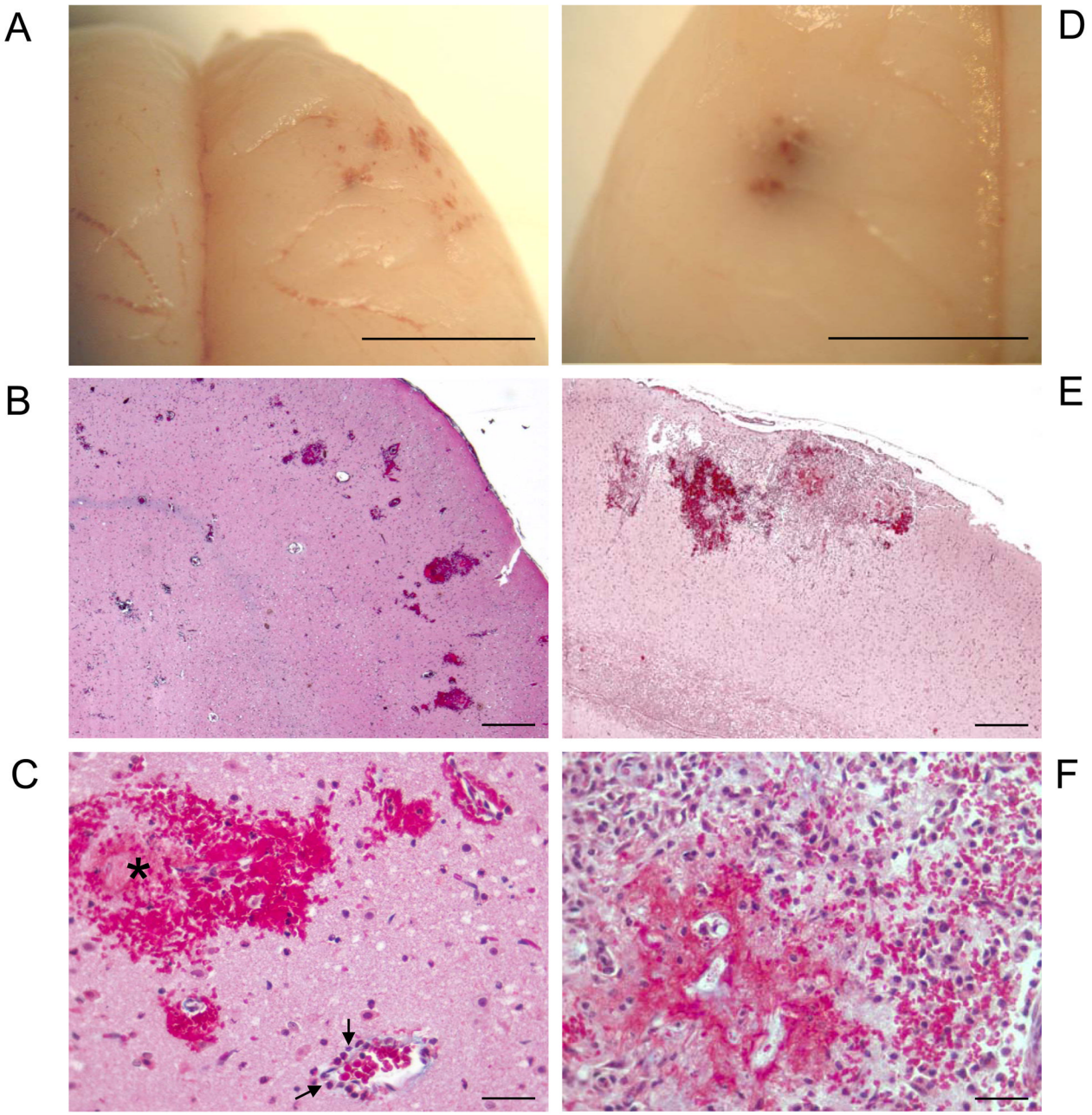

Figure 2.

Representative Stroke+ Rat Brain with Acute (A–C), and Acute+Subacute (D–F) Intracerebral Hemorrhages

(A) Gross inspection of multiple hemorrhagic lesions in right frontal lobe. (B) Microscopic analysis of multiple intracerebral hemorrhages, Masson-trichrome stain. (C) Cortical microhemorrhages and hemorrhagic-infarction (*), transmigrated neutrophils (➔) viewed at higher magnification in Figure 3A, Masson-trichrome stain. (D) Gross inspection of hemorrhage in the left temporal lobe. (E) Microscopic analysis of hemorrhagic-necrotic lesion and inflammatory response, Masson-trichrome stain. (F) High power magnification of

panel-E showing area of hemorrhagic-necrotic lesion and inflammatory response. Scale bar = 5 mm A, D; 400 micron B, E; 25 micron C, F.

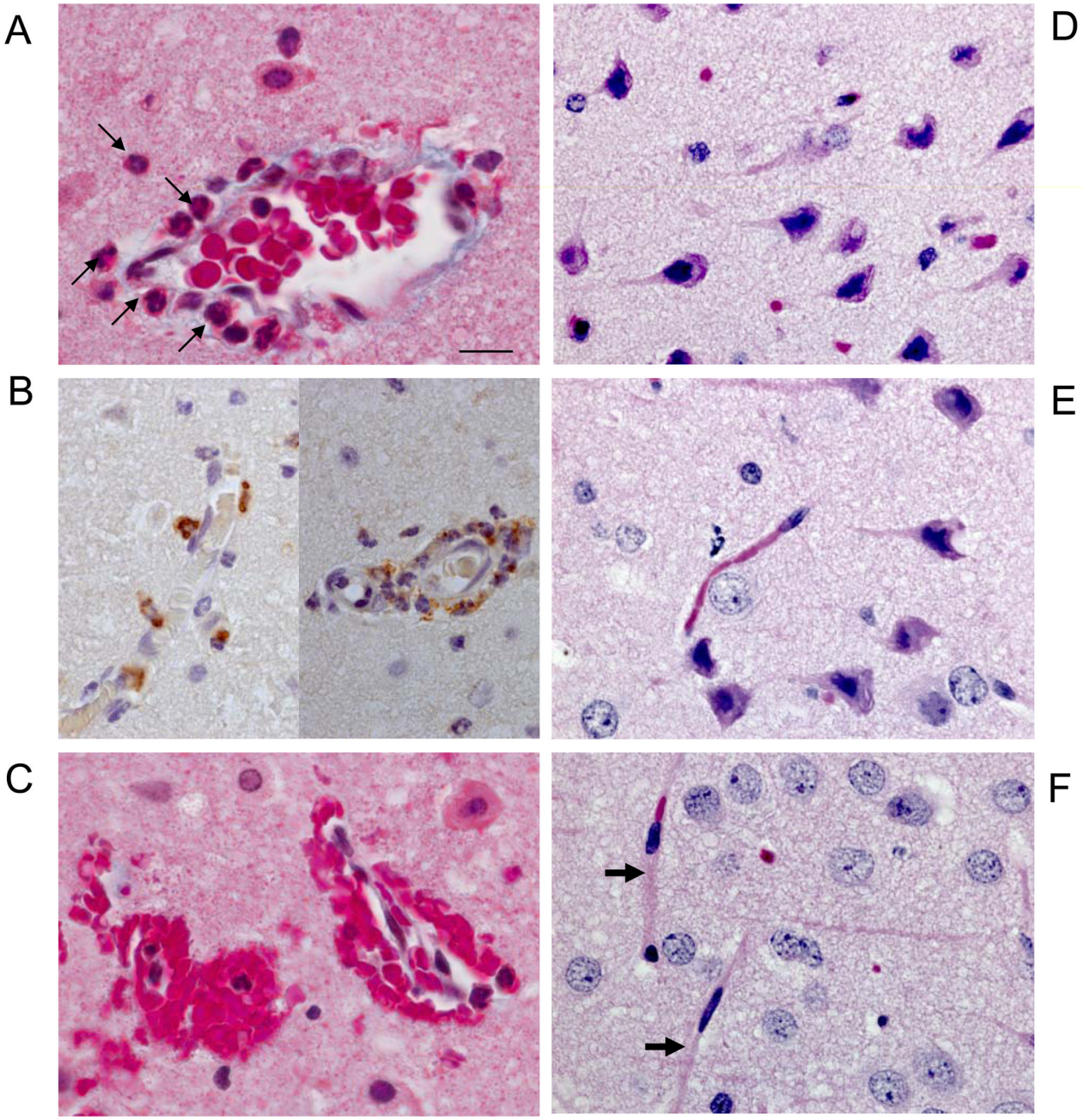

Figure 3.

Analysis of Vascular and Neuronal Alterations in Areas of Microhemorrhages

(A) Representative cortical blood vessel exhibiting neutrophil (➔) transmigration located in area of acute intracerebral hemorrhage shown in Figure 2C; Masson-trichrome stain. (B) Representative myeloperoxidase+ immunostaining (brown) of neutrophils transmigrating through cortical microvessels in area of microhemorrhage without evidence of edema; nuclei are counterstained blue. (C) Masson trichrome-stained section showing microhemorrhages with associated neutrophils. (D–E), Microscopic analysis of surrounding areas of microhemorrhages detects neuronal pyknosis and eosinophilia, microvessel paucity and

microvacuolation, Masson-trichrome stain. (F) Non-affected area with normal neurons and microvessels (→). Scale bar = 10 micron A–F.

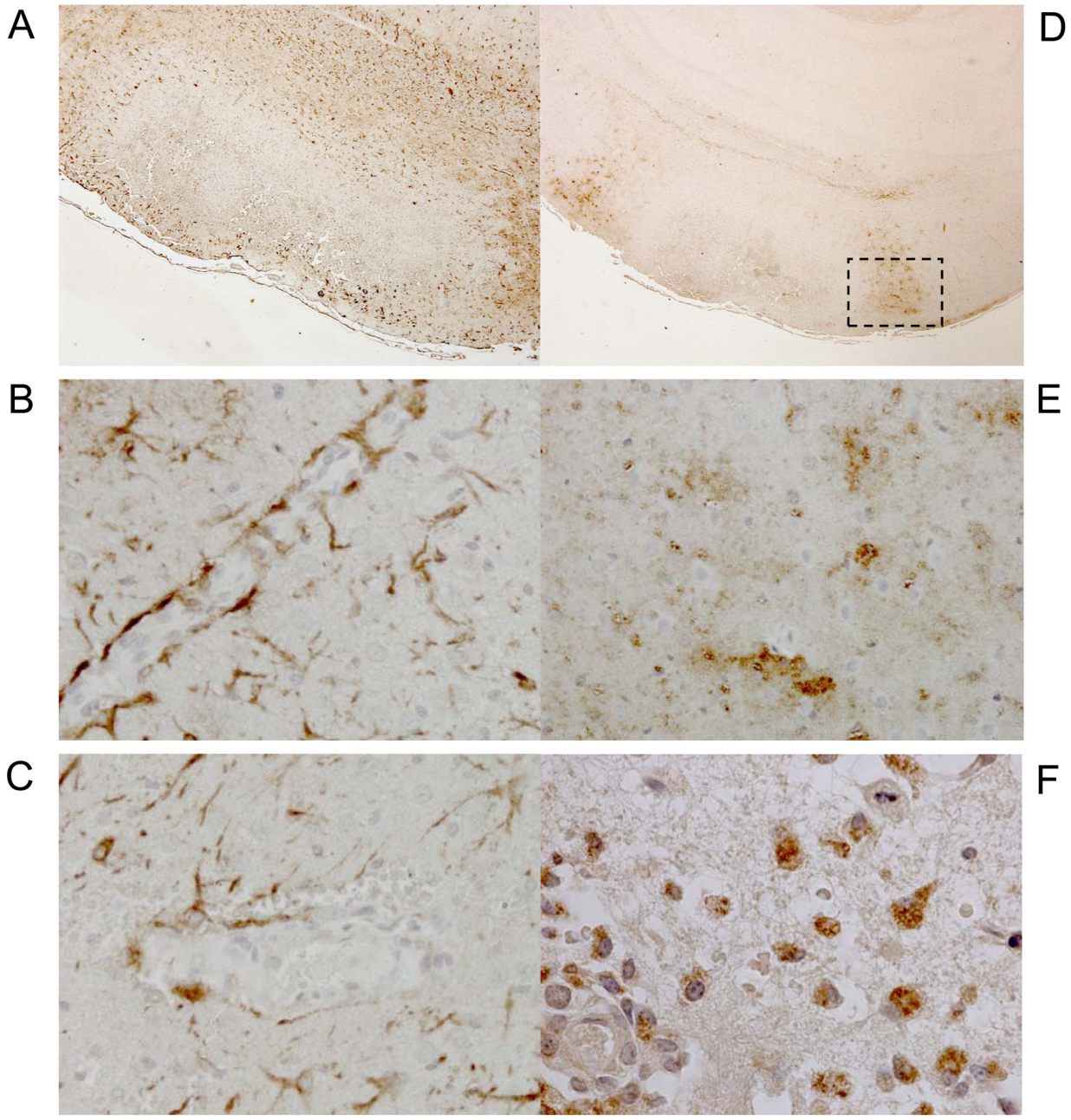

Figure 4.

Immunohistochemical Analysis of Putative Pathogenic Pathways

(A) Glial fibrillary acidic protein (GFAP)-immunostained (brown) astrocytes surround hemorrhagic-necrotic lesion. (B) High magnification of panel A shows contiguous GFAP+ astrocyte endfeet in cortical vessel with no microhemorrhage or neutrophil transmigration. (C) Non-contiguous GFAP-immunostained astrocyte end-feet in cortical blood vessel with microhemorrhage. Erythrocytes and nuclei are counterstained blue-grey. (D) Subacute intracerebral hemorrhagic-necrotic lesion flanked by myeloperoxidase-immunostained (brown) areas. (E) Myeloperoxidase-immunostained (brown) neuropil flanking hemorrhagic-necrotic lesion shown in boxed area in panel-D. (F) High magnification of

immunostained boxed-area in panel-D detects myeloperoxidase-immunostained (brown) monocytes/macrophages. Scale bar=200 microns (A, D); 25 microns (B, C, E); 10 microns (F).

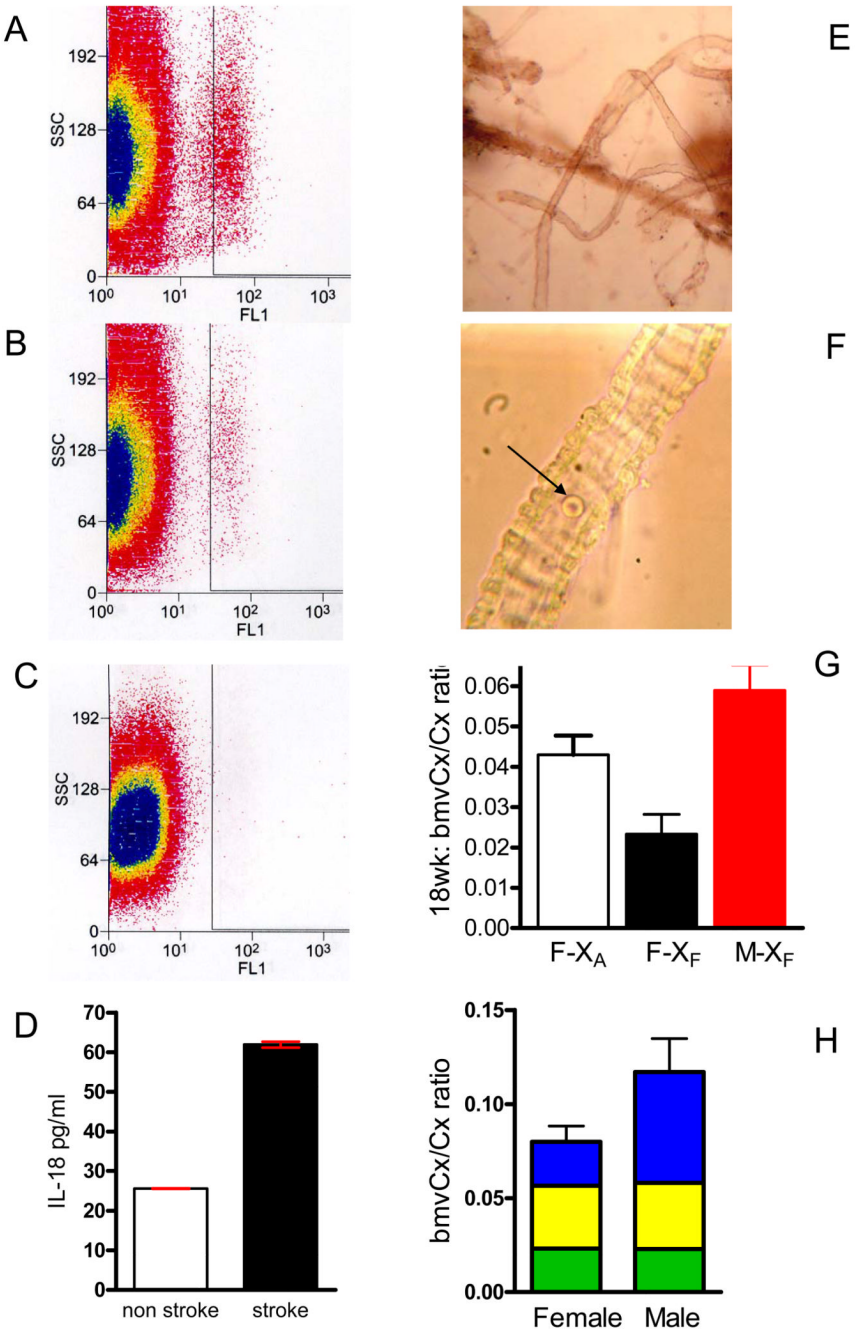

Figure 5.

Systemic Inflammation and Microvascular Paucity

Representative FACS analysis of CD11b+ leukocytes gated for FITC-fluorescence (FL1) and granularity-related side scatter (SSC) comparing (A) X_FTg25-female rat at onset of stroke (n=7), (B) age-matched, pre-stroke X_FTg25-female (n=7), and (C) isotype control. (D) Interleukin-18 plasma levels at the onset of stroke in X_FTg25-females, n=7 (■) compared to age-matched, pre-stroke [X_F]Tg25-female rats, n=7 (□), mean ± sem, two-tailed t-test $P<0.0001$. (E) Isolated brain microvessels. (F) High magnification view of brain microvessel with single red blood cell (→) to depict relative size. (G) Bar graph of total mass of isolated cerebral cortex (cx) brain microvessels (bmv) relative to weight of cerebral

cortex at 4–4.5m of age (mean ± sem; ANOVA $P<0.015$; Tukey's pairwise multiple comparison $P < 0.05$). F, Tg25-female; M, Tg25-male; X_F, fetal 0.4%Na-exposure; X_A, adult-onset 0.4%Na-exposure. X_A Tg25-females (□, n=5); X_FTg25-females (■, n=3), X_FTg25-males (■, n=8). (H) Bar graph depicting bmvCx/Cx ratio (mean ± sem) of X_FTg25-rats at 2 months (■, n=8 females, 10 males), 3-months (■, n=8 females and males), and at 4 to 4.5 m (■, n=3 females, 8 males), mean ± sem. Two-way ANOVA [sex x age] interaction $P < 0.0001$; sex contributes 14.8% of variance with $P=0.0004$; age contributes 21.4% of variance with $P=0.0002$.

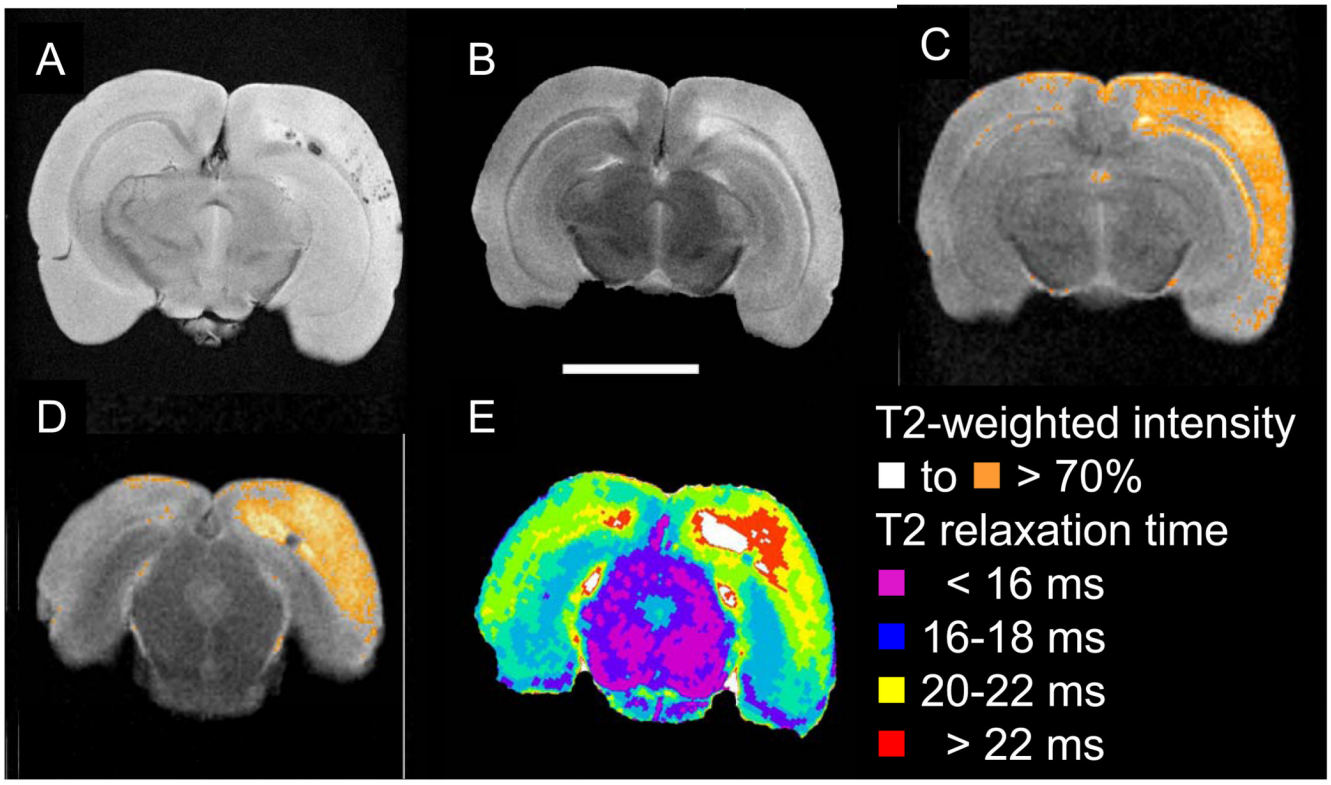

Figure 6.

Representative ex-vivo high-resolution MRI of representative stroke+ brain detects cerebral hemorrhages and microhemorrhages within ischemic area. (A) Axial image of gradient recalled echo sequence detects hemorrhage in the subcortical white matter, and multiple hemorrhages in the cerebral cortex. (B) T2-weighted image detects a relatively extensive region of abnormal, high signal. (C, D) Two representative slices showing quantification of intensity of T2-weighted image highlighting pixels with intensity above 70% of maximal signal depicts area of ischemia following the arterial distribution of the middle cerebral artery. (E) Parametric map showing T2-relaxation within the tissue using a CPMG sequence. The core area of the lesion is depicted with prolonged T2 relaxation times (white-red) which is less extensive than the area indicted on the T2 weighted images (C,D).

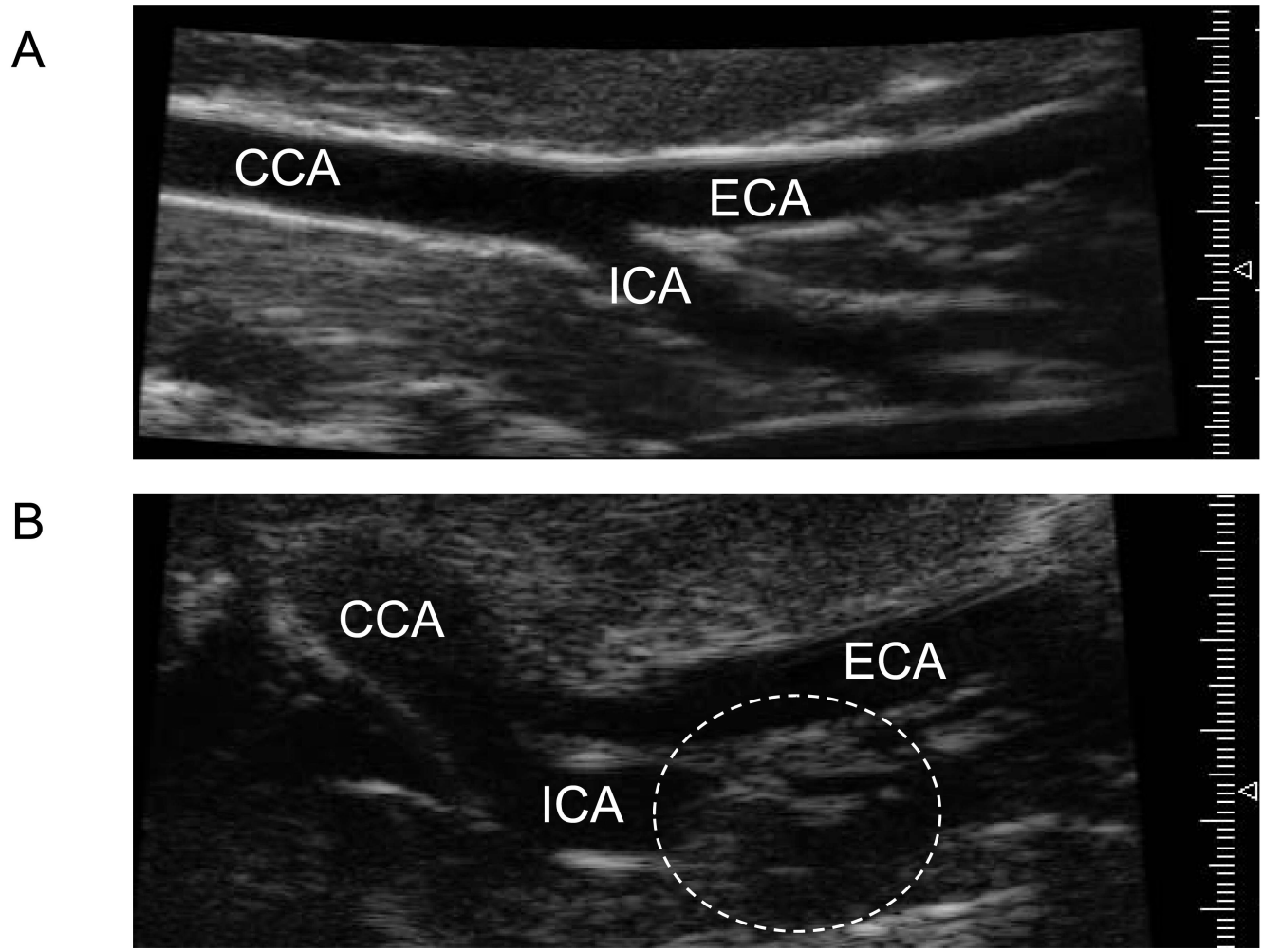

Figure 7.
Representative high-resolution ultrasound microimaging detects carotid artery disease at stroke onset in stroke prone rats. (A) Ultrasound image of control age-matched non-stroke prone (C_F) female showing no lesions or occlusion in common carotid artery (CCA), external (ECA) or internal carotid artery (ICA). (B) Ultrasound image of X_F-stroke-prone Tg25-female at the onset of stroke depicting an occlusive carotid artery lesion (dotted circle) in the ICA.